High-affinity augmentation of endothelial cell attachment: Long-term effects on focal contact and actin filament formation

Anshu B. Mathur, Bernard P. Chan, George A. Truskey, William M. Reichert
Center for Cellular and Biosurface Engineering and Department of Biomedical Engineering, Duke University, Box 90281, Durham, North Carolina 27708-0281

Received 4 June 2002; revised 4 September 2002; accepted 6 September 2002

Abstract: Coadsorption of high-affinity avidin with lower affinity cell adhesion protein fibronectin has been shown to significantly augment short-term (1 h) adhesion and spreading of endothelial cells; however, the longer term persistence of avidin binding and its effect on endothelial cell adhesion have not been addressed. In this study, the presence of avidin–biotin bonds 24 h after cell adhesion to the dual ligand surfaces was verified by laser confocal microscopy of a fluorescent avidin analog, streptavidin. Total internal reflection microscopy showed that the focal contact area, focal contact density, and cell spreading all increased significantly at 24 h compared to fibronectin-treated control surfaces. Focal contact area was identical when measured with cells that were labeled with either the fluorescent streptavidin or a carbocyanine dye incorporated in the cell membrane. Confocal images of stress fibers formed in cells adherent to dual ligand surfaces after 24 h were thicker and more numerous compared to cells adherent to fibronectin controls. The results indicate that 24 h after initial attachment avidin–biotin is localized to focal contacts on the basal surface and affects cell spreading, actin filament organization, and focal contact density. © 2003 Wiley Periodicals, Inc. J Biomed Mater Res 66A: 729–737, 2003

Key words: cell adhesion; focal contacts; cytoskeleton; stress fiber; TIRFM; fibronectin; integrins; avidin; biotin

INTRODUCTION

An approach to improving the patency of synthetic vascular grafts is to seed the graft lumen with a layer of endothelial cells.[1] The binding of cells to the substrate is mediated by integrins that link to extracellular matrix proteins (ECM), primarily fibronectin, adsorbed to the graft surface.[2,3] Integrin–fibronectin binding at focal adhesions initiates actin filament formation that generates mechanical tension throughout the cell. The interactions between the actin and the focal adhesion complex activate signaling pathways and stabilize the cell on the substrate, control cell morphology, proliferation, and differentiation.[4]

In the short term, the ability of seeded endothelium to be retained at the onset of blood flow depends upon rapid attachment and spreading of cells at the lumenal surface. In the long term, however, seeded endothelium endure high vascular shear stresses through cytoskeletal remodeling land by forming strong adhesions to the underlying ECM. Because cell function is dependent upon the actin–focal adhesion link, the mechanical response of the cell to changing shear stress cannot be regulated without strong anchoring of the cell to the ECM. Thus, the effect of surface properties on cell behavior can be analyzed by studying the cell morphology, cell mechanical properties, and focal adhesion formation on various adhesive surfaces.

We hypothesized that high-affinity avidin–biotin bonds ($K_a = 10^{13}$–10^{15} M^{-1}) would bring biotinylated cell membranes in rapid apposition to surfaces coadsorbed with avidin and fibronectin, thus promoting the formation of lower affinity integrin-mediated focal adhesions ($K_a = 10^6$–10^9 M^{-1}). This concept was demonstrated through the binding of biotinylated bovine aortic endothelial cells (BAEC) to surfaces treated with the dual ligand system.[5–8] The cell seeding efficiency and cell retention after exposure to flow (10–30 dynes/cm^2) of BAEC adherent for 1 h on surfaces containing both fibronectin and avidin were significantly higher than for cells attached by either fibronectin or avidin alone.[4] The short-term adhesion increase of the dual ligand system was accompanied by increases in both focal contact area and the number of ligand–receptor bonds.[6] Force balance modeling of

Correspondence to: W. M. Reichert; e-mail: reichert@duke.edu

BAEC adhesion with the dual ligand system showed that cell detachment under flow conditions was attributed to the extraction of receptors from the membrane.[6]

Even though avidin–biotin was shown to significantly enhance initial endothelial cell adhesion, the effects of avidin at longer adhesion times have not been assessed. At longer times cytoskeleton proteins link to focal contacts, forming stress fibers. Stress fibers appear to stabilize contacts, enabling cells to resist higher shear stresses when exposed to flow.[9] Therefore, we examined the effect of avidin–biotin bonds on focal adhesions and the cytoskeleton 24 h after attachment.

Three cell adhesion systems were used for seeding human umbilical vein endothelial cells (HUVEC) in the current study: fibronectin-mediated (fibronectin), avidin–biotin-mediated (avidin–biotin), and avidin–biotin/fibronectin-mediated (dual ligand). The cells were examined at 24 h on the three surfaces to determine if avidin–biotin bonds were still present, and whether avidin–biotin still exerted an influence on focal contact coverage area, actin organization, and the formation of stress fibers. Focal contact formation and organization were evaluated using total internal reflection microscopy (TIRFM). Regions of membrane substrate contacts with separation distance less than 50 nm were defined as focal contacts. Cell spreading was determined using phase contrast microscopy. Confocal imaging was used to characterize actin filament formation, and to track the formation and location of the high-affinity biotin binding using fluorescent streptavidin, which has similar affinity to biotin.[8] Focal adhesion formation for cells labeled with avidin vs. streptavidin were compared to show that there was no effect of changing the ligand between avidin and streptavidin. The location of the avidin–biotin bonds with respect to the cytoskeleton were determined by confocal imaging of dual labeled streptavidin and actin.

MATERIALS AND METHODS

Cell culture

Human umbilical vein endothelial cells (HUVEC) (Clonetics Inc., Walkersville, MD) were grown to confluence in gelatin-coated T25 flasks with Endothelial Basal Medium, EBM, (Clonetics Inc.) supplemented with Endothelial Growth Medium (EGM) growth factors and fetal bovine serum (Clonetics Inc.). Cells were cultured in an incubator with 95% air/CO_2 at 37°C. Passage 1 to 3 HUVEC, at a cell density of 2×10^5 cells/mL, were subsequently cultured on different ligand coated glass coverslips for 24 h.

For fibronectin-coated slides, a 1.0-mL solution of 15 μg/mL fibronectin was placed on each slide for at least 1 h at room temperature. Flasks containing cells were trypsinized until the cells rounded and detached (2–3 min) and then centrifuged to form a pellet. The cell pellet was dispersed and incubated with 15 μg/mL of Dil C_{18} (Molecular Probes Inc., Eugene, OR) in a 300-mM sucrose solution for 10 min. The cells were subsequently cultured in the supplemented EBM on fibronectin coated glass coverslips for 24 h. The cells were incubated with 2% v/v HEPES buffer in supplemented EBM for 1 h prior to TIRFM measurements to maintain a constant pH during the experiment.

Dual ligand preparation for cell attachment

Cells were anchored via avidin–biotin using a modification of the protocol of Bhat et al.,[10] i.e., avidin was attached to biotinylated cells before they were plated on glass slides adsorbed with biotin–BSA. Confluent HUVEC cultured in a T25 flask were incubated with 5 mg/mL of Dil C_{18} (Molecular Probes Inc.) in a 300-mM sucrose solution for 20 min to label the cell membrane. The cells were washed with DPBS after 20 min and then further modified with dual ligand chemistry. A mixture of 1.1 mg of sulfosuccinimidyl 6-(biotinamido) hexanoate (Pierce, Rockford, IL) and 2 mL of DPBS solution was prepared and placed into a T25 flask containing a confluent monolayer of endothelial cells. The cells were incubated for 30 min with the prepared mixture and then washed three times with DPBS. A mixture of 2 mL of DPBS and 20 μL avidin solution was added to the cells. Cells were incubated for 40 min at room temperature. To image the avidin–biotin bond, a solution of 2 mL DPBS with 20 μL streptavidin labeled with Alexa Fluor 488 (Molecular Probes) was incubated for 40 min with the biotinylated cells instead of avidin. Afterwards, the avidin or streptavidin solution was removed and the cells were washed three times with DPBS. After the modification, the cells were allowed to recover overnight with regular growth media.

Flasks with cells ready for seeding were washed with DPBS and trypsinized, centrifuged at 1300 rpm, and resuspended in media. Sterile thin glass coverslips (2.2×7.5 cm) were treated with the solution for the proper coating, given the condition tested. For slides coated with 2 mg/mL BSA:biotin–BSA (ratio 3:1), 167 μL of solution supplemented to 1 mL with DPBS was added for at least 1 h. Slides coated with both fibronectin and BSA:biotin–BSA (dual ligand) were covered for at least 1 h with a solution containing 167 μL of BSA:biotin–BSA and 0.83 mL of 15 μg/mL fibronectin in DPBS solution. Cell viability was measured after 5 days of growth using trypan blue stain. The dual ligand linked cells were $87 \pm 2\%$ ($n = 4$) viable after 5 days in culture on glass coverslips as measured by the trypan blue staining.

Using the HABA (4′-hydroxyazobenzene-2-carboxylic acid) assay,[6,8] membrane biotin concentration was measured at intervals over 45 min. HABA and avidin form a complex that dissociates in the presence of biotin. A water soluble *N*-hydroxy succinimide–ester-derivatized biotin was used to form an amide bond with the lysine residues in the cell membrane of HUVEC in solution.[11] The biotinylated cell solution was added to the HABA–avidin solution of known concentration and changes in absorption at 500 nm were measured using a spectrophotometer. The absorption

changes as avidin dissociates with HABA and binds to biotinylated cells. The number of cells in the flask (hemacytometer count) was counted to determine the amount of molecules of biotin per cell. The calculated value was found to be 1.71×10^9 biotin molecules/cell ($n = 1$).

BSA control experiments

To examine the effect of BSA on HUVEC adhesion to protein-preadsorbed glass slides, a series of cell retention control experiments were conducted in which avidin was not used, and neither the cells nor the adsorbed protein were biotinylated. HUVEC suspended in serum-free EBM were seeded for 1 h onto glass slides adsorbed with either fibronectin or with a mixture of fibronectin and BSA. Percent cell retention was measured using a previously described laminar flow cell[1] that subjected the seeded HUVEC to a range of shear stresses of 1–22 dynes/cm^2. The shear stress at which 50% of the seeded HUVEC were retained (critical shear stress) was determined using a previously described protocol.[10] Protein surface densities of the adsorbed fibronectin and BSA were measured by gamma counting of ^{125}I-labeled BSA and fibronectin using a previously reported protocol.[12]

Actin staining

Endothelial cells adherent to fibronectin and the dual ligand surfaces were stained with rhodamine–phalloidin. For fluorescence staining of the actin, HUVEC cultured for 24 h were immersed in Histoprep Buffered 10% formalin (Fisher Scientific, Pittsburg, PA) to fix the cells. After 10 min, formalin was aspirated and 5 mL of acetone was added at −20°C for 3 min. Permeabilized cells were washed with PBS and 0.6 μg/mL of rhodamine–phalloidin (Sigma Chemicals, St. Louis, MO) in PBS was added to the slide to label actin filaments. The cells were subsequently imaged using confocal microscopy. Images of the stress fibers were quantified by obtaining a line profile of the filaments and then counting the intensity peaks that coincided with the stress fibers. Stress fibers were further characterized by determining the thickness of the bands. Regions of actin clustering or actin nodules were also counted per cell.

TIRFM imaging

The cells were incubated with 2% v/v HEPES buffer in supplemented EBM for 1 h prior to TIRFM measurements to maintain a constant pH during the experiment. The slide was mounted onto a fluid cell after its bottom was dried with lens paper. A 4.1 × 4.7-cm anodized aluminum plate milled with a 3.8 × 1.8-cm opening and 0.1-cm thickness was sealed to the cell plated coverslip surface by a layer of silicon lubricant (Dow Corning Corp., Midland, MI) and then secured to the 12.3 × 7.2-cm fluid cell with screws.[13] This produced a 0.2-cm deep liquid reservoir into which growth media containing HEPES buffer was added to maintain cell viability. The left end of the slide was cleaned with lens paper immersed in 70% ethanol to remove growth media and cell debris from the surface. A small drop of coupling oil (Cargille mineral oil, $n = 1.515$, Cargille labs Inc., Cedar Grove, NJ) was placed on one end of the coverslip to accommodate the coupling prism (BK-7 glass, $n = 1.51$, Karl Lambretch Corp., Chicago, IL). The entire assembly was fixed to the stage of the TIRFM apparatus.[13]

The theory of TIRFM[14] and its application to the study of cell adhesion are described in detail elsewhere.[13] The following approximate expression describes the distance-dependent TIRFM image intensity of an anchorage dependent cell with a fluorophore-labeled cell membrane,

$$F(x,y,\theta_i) = KT_{\text{eff}}(\theta_i)\exp[-\Delta(x,y)/d_{\text{eff}}(\theta_i)]$$

where K is an experimental constant, $T_{\text{eff}}(\theta_i)$ and $d_{\text{eff}}(\theta_i)$ are the effective Fresnel transmission coefficient and depth of penetration of the evanescent wave, respectively, and $\Delta(x,y)$ is the separation distance between the membrane and the substrate. T_{eff} and d_{eff} are a function of the effective refractive index, n_{eff} (1.36) of the anchored cell ($n_{\text{eff}} = n_g\sin(\theta_c)$) ($n_g = 1.517$ and $\theta_c = 66°$), the incidence angle θ_i, and the wavelength of light, λ. In a given experiment, θ_i and n_{eff}/n_g were considered fixed, making $T_{\text{eff}}(\theta_i)$ and $d_{\text{eff}}(\theta_i)$ constants. Point-by-point application of the above relationship via digitized imaging allows one to transform TIRFM data directly into spatial maps of membrane/substrate separation distances.[11,15,16] A nominal separation distance of 31 ± 19 nm was calculated from the slope of linear regression fit of $\ln[F(x,y,\theta_i)/\cos^2\theta_i]$ vs. $1/d_{\text{eff}}(\theta_i)$. The reported separation distance accounts for both focal contact (<15 nm) and close contacts (<50 nm).[16] Subsequent experiments with the TIRFM were conducted at an interfacial angle of 71° because the background interference and contribution from the dorsal membrane were negligible at this angle. The depth of penetration at 71° was calculated to be 85 nm for 488 nm light. Focal contact areas were calculated for focal adhesions within 50 nm to obtain the contact areas of close contacts. Phase contrast images of cells were analyzed using Scion Image 1.62 (www.scioncorp.com) to determine the area projected by the cell perimeter.

Statistical analysis

GraphPad Instat 3.01 (www.graphpad.com) was used to statistically compare data to assess significant variations. One-way ANOVA with Tukey post test was conducted to determine p-values. All data were reported as mean ± SEM with n values given in parenthesis for each.

RESULTS

Similarity of avidin and streptavidin-mediated cell attachment

Focal contact formation in cells adherent to the dual ligand surface in the presence of either avidin or

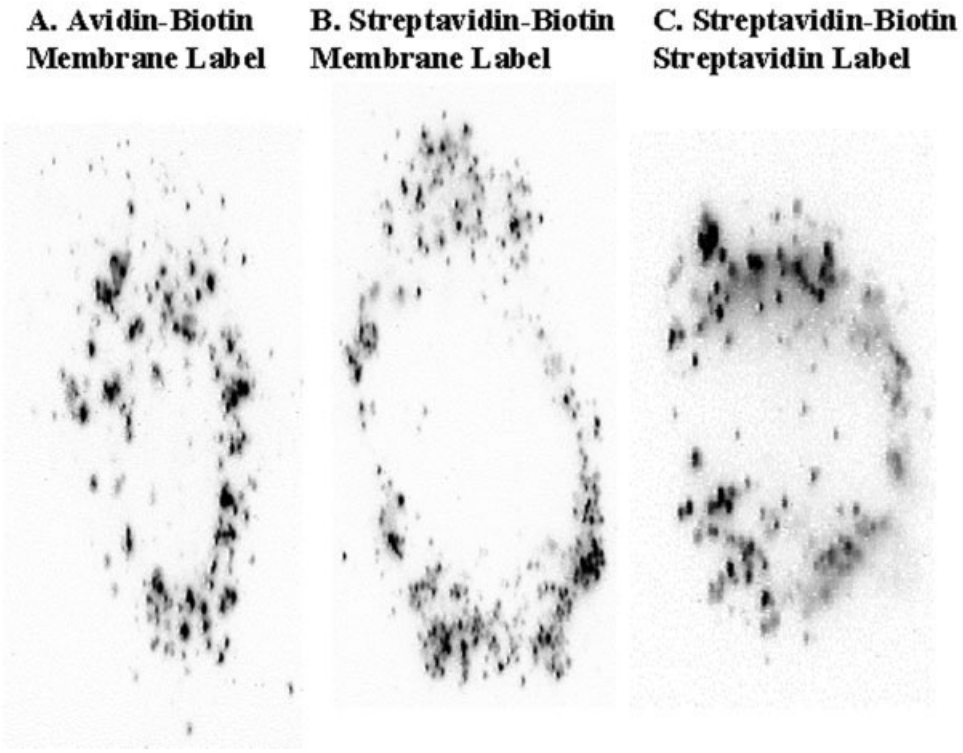

Figure 1. TIRFM imaging of HUVEC focal contacts and streptavidin–biotin bonds appears to be similar for cells adherent to the dual ligand surface.

streptavidin was compared to assess their similarity in adhesion morphology. The TIRFM images in Figure 1 were digitally inverted so that the focal contacts appear as dark spots, and cell–substrate adhesions further away from the substrate are lighter in intensity (gray). The pattern of focal adhesions in the presence of avidin and streptavidin had the same punctate appearance using membrane fluorescent labeling or fluorescently labeled streptavidin. There was no significant difference in the average focal contact coverage area for membrane-labeled cells adherent via the dual ligand system using either avidin–biotin (27.7 ± 3.8 μm^2; $n = 31$) [Fig. 2(A)] or streptavidin–biotin (28.7 ± 5.2 μm^2; $n = 11$) [Fig. 2(B)]. TIRFM of labeled streptavidin showed similar pattern and coverage area (38.0 ± 5.7 μm^2; $n = 20$) [Fig. 2(C)] that was not statistically different than the focal contact coverage area for the membrane labeled cells.

Confocal imaging of streptavidin aggregates and actin filaments

The distribution of streptavidin in cells adherent to dual ligand surfaces were assessed from the z-sectioning of cells using confocal microscopy. Figure 2 shows a series of gray scale confocal z-sections of a single cell from the basal to apical view after 24 h of adhesion. Each 0.4-μm thick section is separated by steps of 0.8 μm. The left column is emission from Alexa-labeled streptavidin. The right column is emission from rhodamine–phalloidin-labeled actin. Streptavidin and actin filaments are present on the apical surface of the cell (top, 2.4 μm), inside the cell (middle, 1.6 and 0.8 μm), and at the basal cell membrane (bottom, 0.0 μm). The largest fraction of streptavidin was present at the basal cell membrane. Because the entire cell was coated with streptavidin, the intracellular, unbound streptavidin may be present on the apical or basal surface of the cell membrane. Streptavidin on the basal surface appears alongside the actin filaments in a similar peripheral pattern seen with TIRFM (Fig. 1).

Figure 3(A) is a confocal image of the basal cell surface after 24 h of adhesion that was dual labeled with Alexa–streptavidin (green) and rhodamine–phalloidin actin filaments (red). The inset shows a streptavidin aggregate located immediately adjacent to an actin filament. Figure 3(B) shows the basal image of another cell after 24 h of adhesion where red actin and green streptavidin emission were superimposed, combining to appear as yellow-orange. The streptavidin clustering with actin in this case appears to occur at terminating ends of the actin filaments, which is consistent with streptavidin colocalization in focal contacts. This observation is in line with the prediction that avidin (or streptavidin) would be present in the region of focal contacts because it accelerates membrane apposition, in turn nucleating integrin-mediated focal adhesion formation. More precise char-

acterization of this colocalization, such as vinculin immunostaining, would be necessary to definitively demonstrate colocalization.

Effect of the dual ligand on stress fiber formation

Figure 4 compares confocal images of rhdamine–phalloidin stained actin after 24 h of adhesion via fibronectin–integrin [Fig. 4(A)] and via the dual ligand treatment [Fig. 4(B)]. Filamentous actin coalesced to form significantly ($p < 0.001$) thicker bands (1.71 ± 0.15 μm, $n = 20$) with the dual ligand compared to the cells on the fibronectin surfaces (0.93 ± 0.11 μm, $n = 20$). The number of stress fibers was significantly higher for the dual ligand (16.9 ± 1.9 fibers/cell, $n = 12$) than for cells adherent to fibronectin (9.1 ± 0.9 fibers/cell, $n = 12$). The number of actin nodules on the dual ligand adherent cells (1.5 ± 0.3 nodules/cell) was also significantly ($p < 0.05$) higher than on fibronectin (0.5 ± 0.2 nodules/cell).

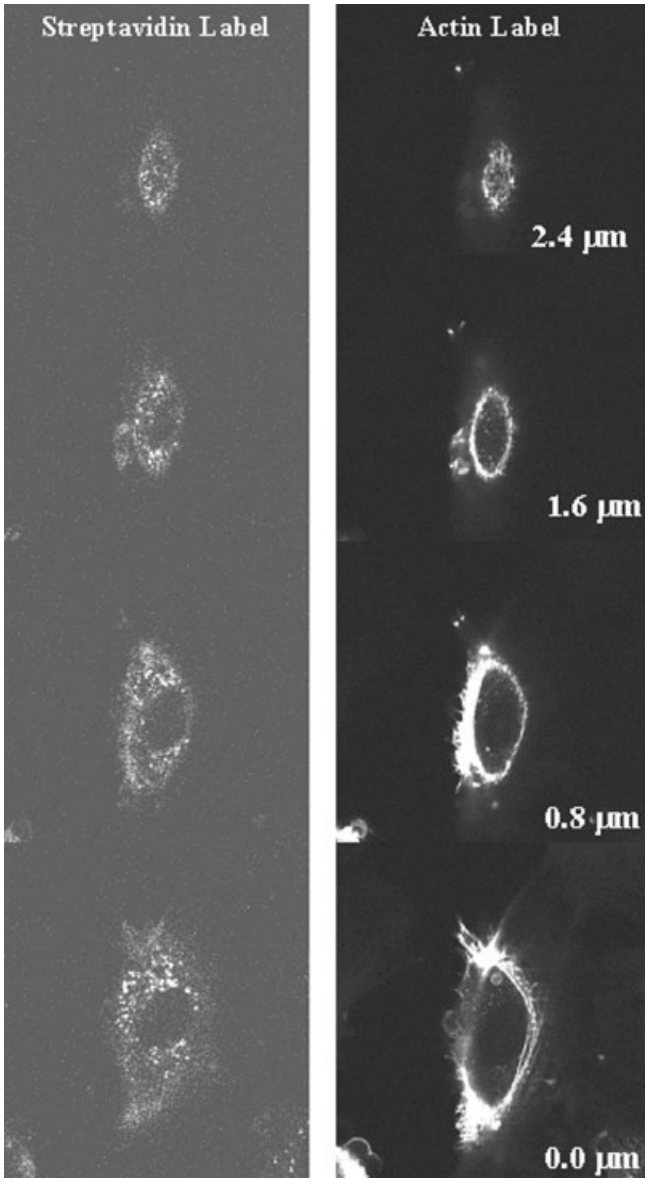

Figure 2. Z-sectioning of streptavidin labeled and actin labeled HUVEC. The images shown above are 0.8 μm apart and are in grayscale. Basal image, 0.0 μm; apical image, 2.4 μm.

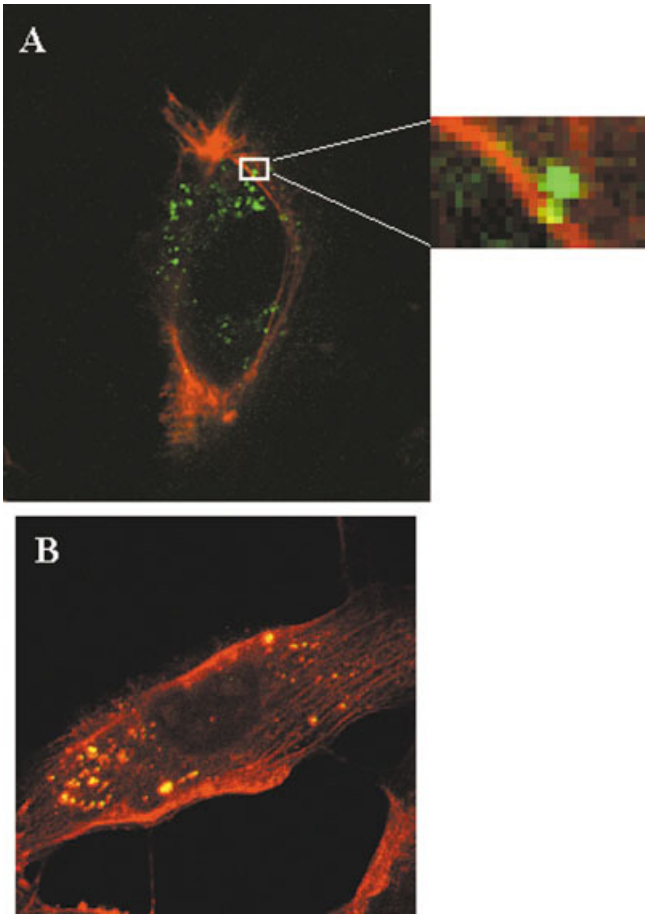

Figure 3. After 24 h of attachment, the streptavidin–biotin bonds appear as green regions and the rhodamine–phalloidin labeled actin filaments are red (A). The regions where actin and streptavidin emission superimposed appear as yellow-orange (B).

Effect of dual ligand binding on focal contact area

Figure 5 compares the TIRF images of HUVEC adherent to the (A) fibronectin surface, (B) dual ligand surface, and (C) avidin–biotin surfaces. The distribution of focal contacts around the cell periphery encircling the central nucleus were similar for cells attached to the dual ligand and the fibronectin surfaces at 24 h. Cells on the dual ligand surface appeared to have a higher density of more intensely dark regions than cells on the fibronectin or avidin–biotin surfaces. In

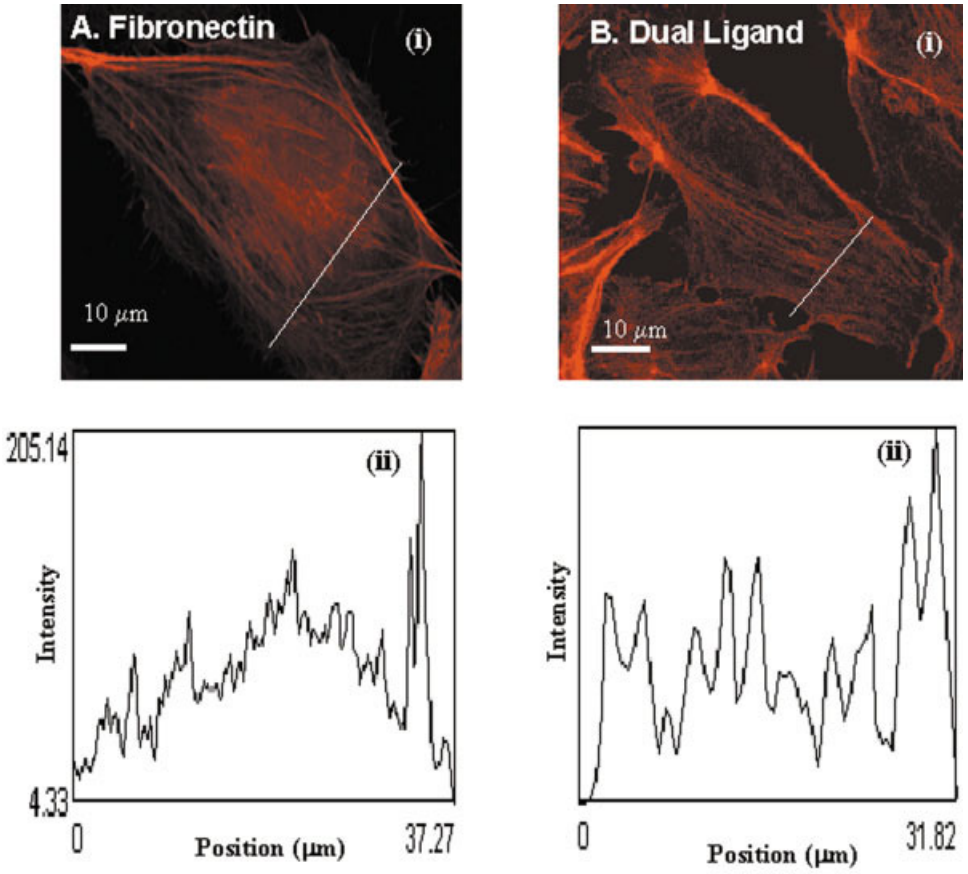

Figure 4. Actin filaments of cells adherent to the (A) fibronectin and (B) dual ligand surfaces span the cell around the central nucleus (i). A line profile across the cell shows the location, number, and the thickness of the stress fibers as indicated by intensity peaks (ii).

addition, focal contacts formed on the avidin–biotin surface were the least dense of all surfaces examined.

Table I provides a quantitative analysis of the focal contact area and cell spread area on the three surfaces. On average, cells adherent to the dual ligand surface had the highest focal contact area, number of focal contacts, projected area (cell spreading), and total focal contact area per projected area, followed by the fibronectin surface, and then the avidin–biotin surface. Only the average area per focal contact and the number of focal contacts per projected area did not fit this trend. The average area per focal contact was similar for the dual ligand and the fibronectin surfaces and lower for the avidin–biotin surface; whereas the number of contacts per projected area was highest for the dual ligand and similar and lower for the fibronectin and avidin–biotin surfaces.

Figure 6 shows the size distribution of focal contacts on the three surfaces that were examined. The vast majority of focal contacts on all surfaces were 5 μm^2 or smaller; however, relative to fibronectin pretreated surfaces, the presence of avidin–biotin bonds increased the number of contacts smaller than 0.25 μm^2 and decreased the number of focal contacts in the 0.25–5 μm^2 range. This result suggests that avidin acts simply to nucleate the formation of focal contacts but does not promote formation of larger contacts. This result may be a function of the avidin density.

Influence of BSA on HUVEC adhesion

The presence of BSA in a mixed monolayer with fibronectin may also assert an influence on the adhesion of HUVEC to protein–preadsorbed glass slides in the absence of biotinylation and avidin. Radiolabeling was used to determine the surface densities of the adsorbed fibronectin and BSA. As shown in Table II, the mixed monolayer was roughly 4:1 BSA to fibronectin, and had three-fourths the surface density of fibronectin compared to the fibronectin-only case. Figure 7 contains the percent retention of HUVEC measured over a range of shear stresses in a laminar flow cell system after 1 h of cell adhesion time. The open symbols are for HUVEC adherent to glass slides preadsorbed with fibronectin. The filled symbols are for HUVEC adherent to glass slides preadsorbed with a mixture of fibronectin and BSA. The critical shear stresses determined from these

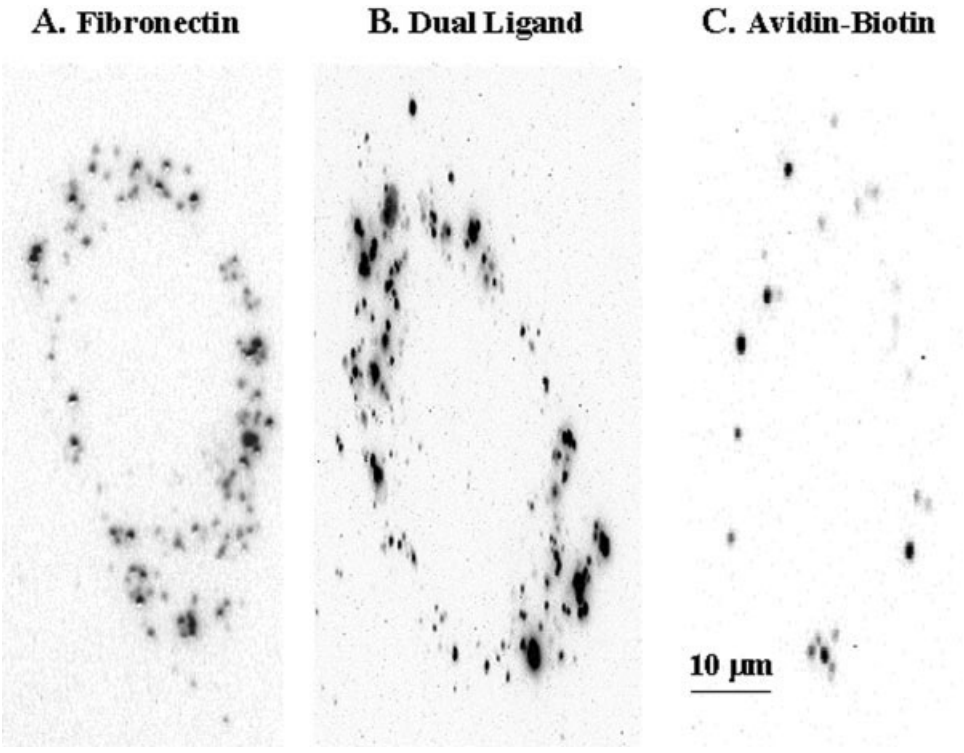

Figure 5. Focal adhesion arrangement of HUVEC adherent to (A) Fibronectin, (B) dual ligand, and (C) avidin—biotin surfaces. The close focal contacts appear as darker spots where as cell-substrate adhesions further away from the substrate are lighter in intensity (gray). On the dual ligand surface the darker regions are most prominent, followed by the fibronectin surface and lastly the avidin–biotin surface.

data were 10 ± 1.8 dynes/cm^2 for fibronectin only, and 12 ± 2.5 dynes/cm^2 for the mixed monolayer. Using a paired Student's *t*-test, these two sets of cell retention data were determined to be statistically indistinguishable at the 95% confidence level ($p >> 0.05$).

DISCUSSION

If avidin–biotin merely enhanced cell adhesion in the short term, then one would expect that biotinylated HUVEC after 24 h of attachment on avidin surfaces would not differ from that of cells attached to a fibronectin surface in terms of the cell spread area, focal contact number and size, and actin filament size and density. In the current study, avidin was present throughout the cell at 24 h, but localized to focal contacts on the basal surface. As a result, avidin–biotin bonds persisted in augmenting focal adhesion formation at longer times, and yielded stress fibers that were thicker and more numerous compared to cells adherent to fibronectin controls.

TABLE I
Average Values of Focal Contact Measurements for the Three Different Ligand Systems

	Fibronectin	Dual Ligand	Avidin–Biotin
Total focal contact area per cell (μm^2)	10.6 ± 1.6 (n = 16)	27.7 ± 3.8** (n = 31)	4.02 ± 0.52**††† (n = 17)
Number of Focal Contacts per cell	42.3 ± 4.2 (n = 19)	109.0 ± 11.1*** (n = 27)	29.7 ± 3.0††† (n = 19)
Projected area per cell (μm^2)	647 ± 41 (n = 21)	831 ± 86* (n = 26)	391 ± 38*††† (n = 23)
Focal contact area per projected cell area	0.016 ± 0.002 (n = 16)	0.033 ± 0.01* (n = 26)	0.010 ± 0.002††† (n = 17)
Number of contacts per projected cell area (μm^{-2})	0.065 ± 0.007 (n = 19)	0.13 ± 0.02* (n = 26)	0.076 ± 0.01† (n = 19)
Average area per focal contact (μm^2)	0.24 ± 0.05 (n = 16)	0.25 ± 0.03 (n = 27)	0.14 ± 0.03***††† (n = 17)

***, **, * indicates $p < 0.001$, $p < 0.01$, and $p < 0.05$, respectively, compared to fibronectin and †††, ††, † indicates $p < 0.001$, $p < 0.01$, and $p < 0.05$, respectively, compared to the dual ligand.

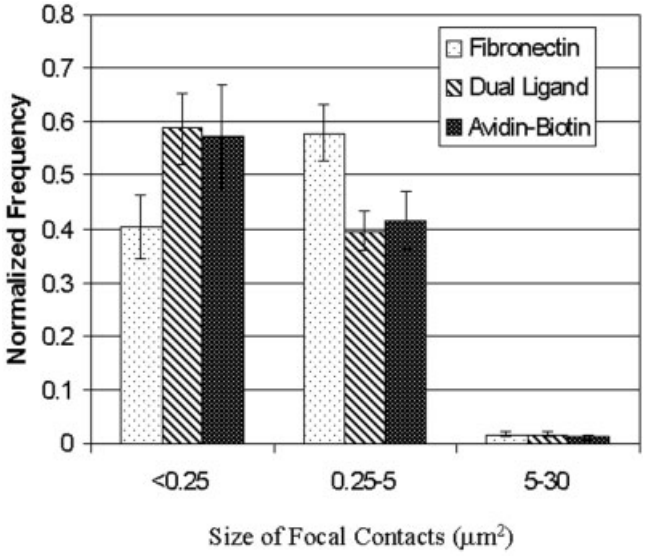

Figure 6. The average normalized frequency of focal contacts size distribution shows that there was a wide range of sizes for focal contacts of cells adherent to fibronectin, dual ligand, and avidin–biotin surfaces.

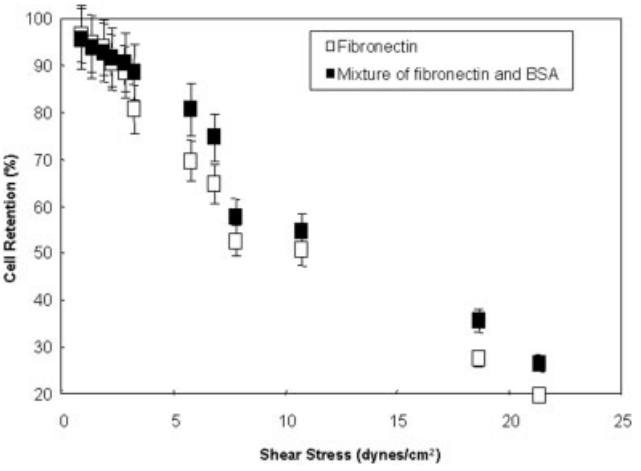

Figure 7. Effect of BSA on the adhesion of HUVEC onto surface preadsorbed with fibronectin or preadsorbed with a mixture of BSA and fibronectin. The two data sets are statistically indistinguishable at the 95% confidence level.

Bhat et al.[5] found an increase in cellular contact area of BAEC after 1 h of adhesion for cells adherent with the dual ligand versus the fibronectin ligand, which had a greater contact area than the avidin–biotin ligands alone. What we show is that this trend persisted after 24 h of adhesion for HUVEC. A small increase in cellular spreading after 24 h was evident for HUVEC adhesion on the dual ligand surface compared to the fibronectin adherent cells. The persistence of a similar trend after 24 h indicates that the dual ligand binding is capable of further enhancing adhesion.

The pattern of focal adhesion formation at 24 h for avidin–biotin (and streptavidin–biotin) surfaces showed a peripheral and punctate distribution similar to that observed on the dual ligand surface and fibronectin only surfaces; however, there were significant quantitative differences. Although the total focal contact area per cell for the dual ligand surface was more than twice that observed for cells on fibronectin, the average size of the focal contacts was the same. Similarly, the focal contact area of dual ligand adherent cells was more than four times higher than for avidin–biotin, with the average size of the focal contacts also being higher. The number of focal contacts per cell on the dual ligand surface was more than twice that of fibronectin and slightly more than three times higher than on avidin–biotin. These results suggest that the rapid anchoring of the biotinylated membrane to surface locations of avidin–biotin binding nucleates the formation of integrin–fibronectin bonds in the immediate vicinity, thus augmenting natural cell adhesion by promoting integrin clustering.[17]

TABLE II
Surface Densities (±SD) of Adsorbed ^{125}I Labeled Fibronectin and BSA (10^{11} Molecules/cm^2)

	Fibronectin Preadsorption	Fibronectin and BSA Preadsorption
Fibronectin surface density	1.4 ± 0.1	1.1 ± 0.1
BSA surface density	—	4.7 ± 0.8

This increase in focal contact area affected stress fiber formation of HUVEC. Because the focal adhesions are links between the cytoskeleton and the substrate, an increase in focal adhesions would lead to an increase in actin polymerization and stress fiber formation. Previously, cell adhesion was studied on surfaces coated with varying fibronectin densities of 10–500 ng/cm^2.[18] An increase in the substrate coating density of fibronectin resulted in an increase in cell spreading by fivefold. The increase in cell spreading and cytoskeletal properties was attributed to the focal adhesion formation. Our results corroborate these findings that the introduction of a high-affinity ligand at the focal contacts increases the area occupied by focal contacts and affects the actin stress fiber properties.

Cell adhesion appeared to be affected by the addition of the avidin–biotin bonds because it influenced focal adhesion and stress fiber formation of human endothelial cells. For focal adhesions to form, the clustering of integrins at the adhesive sites is an important first step.[17] As the integrins assemble in focal contacts, the cytoplasmic portion of the β-domain of the integrins associates with the actin filaments resulting in stress fiber formation. The association of the integrins on one end with the adhesion protein on the substrate and on the other end with the actin filaments is a positive feedback mechanism, which could result in

formation of larger stress fibers. Therefore, as the avidin–biotin bonds are introduced along with the integrin–fibronectin bonds, the increase in focal adhesions acts as a positive feedback mechanism that promotes stress fiber formation.[17]

This study also included a set of cell retention control experiments that examined whether BSA itself affects HUVEC adhesion in the presence of fibronectin after 1 h of cell seeding. There are three possible outcomes with respect to the presence of BSA used in the dual ligand cell adhesion protocol. First, BSA in the mixed monolayer may diminish the ability of fibronectin to promote integrin-mediated cell adhesion through a depletion effect. Second, the BSA may augment HUVEC adhesion, possibly by altering fibronectin conformation as reported by Grinell and Feld.[19] Third, BSA may have no effect and act primarily as a noninteractive protein. As shown in Figure 7, there was no statistical difference between the adhesion of HUVEC to substrates preadsorbed with fibronectin or preadsorbed with a mixture of fibronectin and BSA. Therefore, the presence of BSA neither augmented nor inhibited the ability of fibronectin to promote HUVEC attachment in the critically sensitive first hour of cell adhesion.

CONCLUSIONS

This study showed that the avidin–biotin bonds in the presence of integrin–fibronectin bonds at 24 h augmented total area and density of focal contacts, although avidin–biotin bonds by themselves do not produce this effect. The higher density of focal contacts on the dual ligand surface indicates that focal contacts were more prominent on the dual ligand surface due to the presence of both integrin dependent and integrin independent bonds. Thus, it is important that the avidin–biotin bonds are used to support, but not supplant, the fibronectin–integrin adhesion mechanism. Under shear stress conditions, one of the ways the cells reduce the force acting over their apical surface is by developing stress fibers.[20] Introduction of avidin–biotin bonds at the cell–substrate interface enhanced focal contact formation and cell spreading, which altered the stress fiber formation. The cell configuration (thicker stress fibers coupling with large number of focal adhesions) adopted on the dual ligand surface would allow the cells to bear high shear stresses under flow conditions.

References

1. Pollara P, Allessandri G, Bonardelli S, Simonini A, Cabibo E, Portolani N, Tiberio GA, Giulini SM, Turano A. Complete in vitro prosthesis endothelialization induced by artificial extracellular matrix. J Invest Surg 1999;12:81–88.
2. Maniotis AJ, Chen CS, Ingber DE. Demonstration of mechanical connections between integrins, cytoskeletal filaments, and nucleoplasm that stabilize nuclear structure. Proc Natl Acad Sci USA 1997;94:849–854.
3. Davies PF. Flow-mediated endothelial mechanotransduction. Physiol Rev 1995;75:519–560.
4. Garcia AJ, Boettiger D. Integrin–fibronectin interactions at the cell–material interface: Initial integrin binding and signaling. Biomaterials 1999;20:2427–2433.
5. Bhat VD, Klitzman B, Koger K, Truskey GA, Reichert WM. Improving endothelial cell adhesion to vascular graft surfaces: Clinical need and strategies. J Biomater Sci Polym Ed 1998;9: 1117–1135.
6. Chan BP, Bhat VD, Yegnasubramanian S, Reichert WM, Truskey GA. An equilibrium model of endothelial cell adhesion via integrin-dependent and integrin-independent ligands. Biomaterials 1999;20:2395–2403.
7. Savage MD. Avidin–biotin chemistry: A handbook. Rockford, IL: Pierce Chemical Company; 1994.
8. Alberts B, Bray D, Lewis J, Raff M, Roberts K, Watson JD. Molecular biology of the cell. New York: Garland Publishing, Inc.; 1994.
9. Ward MD, Hammer DA. A theoretical analysis of the effect of focal contact formation on cell-substrate attachment strength. Biophys J 1993;64:936–956.
10. Bhat VD, Truskey GA, Reichert WM. Using avidin-mediated binding to enhance initial endothelial cell attachment and spreading. J Biomed Mater Res 1998;40:57–65.
11. Levy-Toledano R, Caro HL, Hindman N, Taylor S. Streptavidin blotting: A sensitive technique to study cell surface proteins: Application to investigate autophosphorylation and endocytosis of biotin-labeled insulin receptors. Endocrinology 1993;133:1803–1808.
12. Truskey GA, Pirone JS. The effect of fluid shear stress upon cell adhesion of fibronectin-treated surfaces. J Biomed Mater Res 1990;24:1333–1353.
13. Mathur AB, Truskey GA, Reichert WM. Atomic force and total internal reflection fluorescence microscopy to study force transmission in endothelial cells. Biophys J 2000;78:1725–1735.
14. Reichert WM, Truskey GA. Total internal reflection fluorescence (TIRF) microscopy I. Modeling of cell contact region fluorescence. J Cell Sci 1990;96:219–230.
15. Burmeister JS, Truskey GA, Reichert WM. Quantitative analysis of variable-angle total internal reflection fluorescence microscopy (VA-TIRFM) of cell/substrate contacts. J Microsc 1994;173:39–51.
16. Burmeister JS, Olivier LA, Reichert WM, Truskey GA. Application of total internal reflection fluorescence microscopy to study cell adhesion to biomaterials. Biomaterials 1998;19:307–325.
17. Giancotti FG, Ruoslahti E. Integrin signaling. Science 1999;285: 1028–1032.
18. Wang N, Ingber DE. Control of cytoskeletal mechanics by extracellular matrix, cell shape, and mechanical tension. Biophys J 1994;66:2181–2189.
19. Grinnell F, Feld MK. Fibronectin adsorption on hydrophilic and hydrophobic surfaces detected by antibody-binding and analyzed during cell-adhesion in serum-containing medium. J Biol Chem 1982;257:4888–4893.
20. Barbee KA, Davies PF, Lal R. Shear stress-induced reorganization of the surface topography of living endothelial cells imaged by atomic force microscopy. Circ Res 1994;74:163–171.